introduce a vinylbenzyl group in alkali solution with tetrabutylphosphonium bromide as a phase transfer catalyst. The respective vinylbenzyl group-terminated NIPAAm, NVA, and BMA macomonomers were obtained. After dialysis of the macromonomers in a polar solvent, they were lyophilized.

Ionic VAm and MAA macromonomers were prepared by hydrolysis of the corresponding nonionic NVA and BMA macromonomers, respectively, as we reported previously.[19] The nonionic macromonomers were dissolved in strong acid containing hydroquinone as a polymerization inhibitor. After hydrolysis of the macromonomers at 80°C for 12–24 h, ionic VAm and MAA macromonomers were obtained. They were dialyzed in purified water and then lyophilized.

Nanoparticles

Nanoparticles other than those with a crosslinked hydrophobic polystyrene core were prepared by our (conventional) methods.[13,19] The corresponding macromonomers were polymerized with styrene at the predetermined molar ratio in a polar solvent including AIBN (Tables 1 and 2). After the dispersion copolymerization, the resulting nanoparticles were dialyzed to remove unreacted substances and then lyophilized.

To prepare nanoparticles with crosslinked hydrophobic polystyrene cores, divinylbenzene was used as a crosslinking agent. Predetermined amounts of monomers (Tables 1 and 2) were dissolved in 5 mL of ethanol containing 20% (v/v) of purified water. The total weight of monomers was adjusted to 1.0 g. Macromonomers were copolymerized with styrene and divinylbenzene in the presence of AIBN (1 mol% to total monomers) at 60°C for 24 h in a vacuum.[13,19] After the dispersion copolymerization, the resulting nanoparticles were dialyzed to remove unreacted substances and then lyophilized.

Characterization of Nanoparticles

The oligomers, macromonomers and nanoparticles were characterized as described in our earlier articles.[19–24,27–30] Briefly, the number-average molecular weights (M_n) of oligomers and macromonomers were determined by gel permeation chromatography. Hydrolysis of macromonomers and their introduction onto nanoparticles were confirmed by the IR spectra. The nanoparticle size was measured by dynamic light-scattering spectrophotometry (DLS-700, Otsuka Electronics Co., Japan). The zeta potential of PVAm nanoparticles was measured by electrophoretic light-scattering spectrophotometry in phosphate buffer (pH: 7.4; ionic strength: 0.15) at 25°C (ELS-800, Otsuka Electronics Co., Japan).

Animal Experiments

Dosing Solution

The lyophilized nanoparticles were re-dispersed in purified water at a concentration of 20 mg/mL. Human calcitonin was dissolved in purified water at a concentration of 0.2 mg/mL. The nanoparticle aqueous dispersion was mixed with an equivalent volume of hCT aqueous solution. Separately, hCT was dissolved in saline solution at a concentration of 0.4 μg/mL as a dosing solution for subcutaneous administration.

Table 1. Molar ratio of monomers in the preparation of nanoparticles having one kind of surface polymeric chains.

	Molar ratio of monomers			Mn[a]
	Macromonomer	Styrene	Divinylbenzene	
PNIPAAm NPs	1	40	0	3.5
PNVA NPs	1	40	0	15
PMAA NPs	1	40	0	3.9
PVAm NPs	1	40	0	19
	1	5	0	19
	1	10	0	8.5
	1	10	0.15	8.5
	1	10	0.3	8.5
	1	10	0.45	8.5
	1	10	0.6	8.5

[a]Number-average molecular weight of macromonomer ($\times 10^3$).

Table 2. Molar ratio of monomers in the preparation of nanoparticles having two kinds of surface polymeric chains.

	Molar ratio of monomers				Mn[a]
	Macromonomer-1	Macromonomer-2	Styrene	Divinylbenzene	
PVAm–PNIPAAm NPs[b]	0.5	1.5	80	0	19/3.5[c]
	1	1	80	0	19/3.5[c]
	1.5	0.5	80	0	19/3.5[c]
	1.5	0.5	10	0	19/3.5[c]
	1.5	0.5	10	0.3	19/3.5[c]
PVAm–PMAA NPs[b]	1	1	10	0	19/14[c]
	1	1	10	0.3	19/14[c]

[a]Number-average molecular weight of macromonomer ($\times 10^3$).
[b]Macromonomer-1: VAm, macromonomer-2: NIPAAm or MAA.
[c]Left side of slash (/): Mn of macromonomer-1, right side of slash: Mn of macromonomer-2.

Animal Experiment

Animal experiments in this article were approved by local ethical review committees of Daiichi Pharmaceutical Co., Ltd. Seven week-old overnight-fasted male Sprague–Dawley strain rats were used ($n = 5$). The dosing solution was administered orally to rats at a dose of 0.25 mg of hCT and 25 mg of nanoparticles in a 2.5 mL mixture/kg of body weight. As a control, an aqueous solution of hCT (1 mg/mL) was given orally to rats (2.5 mg of hCT in 2.5 mL of purified water/kg of body weight). An hCT saline solution (0.4 μg/mL) was also administered to rats subcutaneously to calculate relative bioavailability (1 μg of hCT in a 2.5 mL of saline solution/kg of body weight). Blood (0.5 mL) was sampled from a jugular vein under ether anesthesia at 0, 5, and 20 min after subcutaneous and oral administration of hCT. The blood was mixed with EDTA and aprotinin, and then it was centrifuged (15,000 rpm, 10 min) to obtain plasma samples.

Measurement of Human Calcitonin Concentration in Plasma Sample

The concentration of hCT in plasma was measured by using specific radioimmunoassay. Radiolabeled hCT (^{125}I-hCT) was prepared by the lactoperoxidase method.[31] A buffer solution containing 0.05 M of Na_2HPO_4, 0.08 M of NaCl, 0.025 M of EDTA.2Na, 0.05 w/v% of NaN_3, and 0.5 w/v% of skim milk was prepared and adjusted to pH 7.4 by the addition of 1 N of NaOH. Rabbit antiserum against hCT was diluted by the buffer solution at a ratio (v/v) of 1:25,600. The plasma sample (100 μL) was incubated with the anti-hCT rabbit serum solution (100 μL) for 24 hr at 4°C. After the addition of 100 μL of ^{125}I-hCT (appropriately 15,000 cpm, dissolved in the buffer solution) and 100 μL of rabbit IgG dissolved in the buffer solution at a concentration of 0.3 mg/mL, the mixture was incubated for 24 hr at 4°C. Separately, anti-rabbit IgG goat serum corresponding to 1 mL of the goat serum was added to 30 mL of buffer solution and subsequently mixed with 30 mL of polyethyleneglycol aqueous solution (20 w/v%, Mw: 2000). Then, 1 mL of this anti-rabbit IgG goat serum solution was added to the plasma-containing mixture and then incubated for 1 hr at 4°C. After incubation, the mixture was centrifuged (3000 rpm, 30 min) and the supernatant was removed by aspiration. Radioactivity of the resulting precipitate (antibody-bound ^{125}I-hCT) was determined with a gamma counter (ARC-1000M, Aloka Co., Japan).

Statistical Analysis

The area under the blood concentration-time curve from 0 to 20 min ($AUC_{0-20\,min}$) was calculated trapezoidally. In this research, relative bioavailability (absorption rate) was defined as the percentage of the ratio of $AUC_{0-20\,min}$ after oral administration of hCT with or without nanoparticles to the dose-corrected $AUC_{0-20\,min}$ after subcutaneous administration of hCT. Statistical significance was assessed with the Student's t-test, and p values of 0.05 or less were considered significant.

RESULTS

Characteristics of Nanoparticles

Figure 1 shows the chemical structure of the nanoparticles. A hydrophobic polystyrene backbone was crosslinked only when divinylbenzene was added in the copolymerization between macromonomers and styrene.

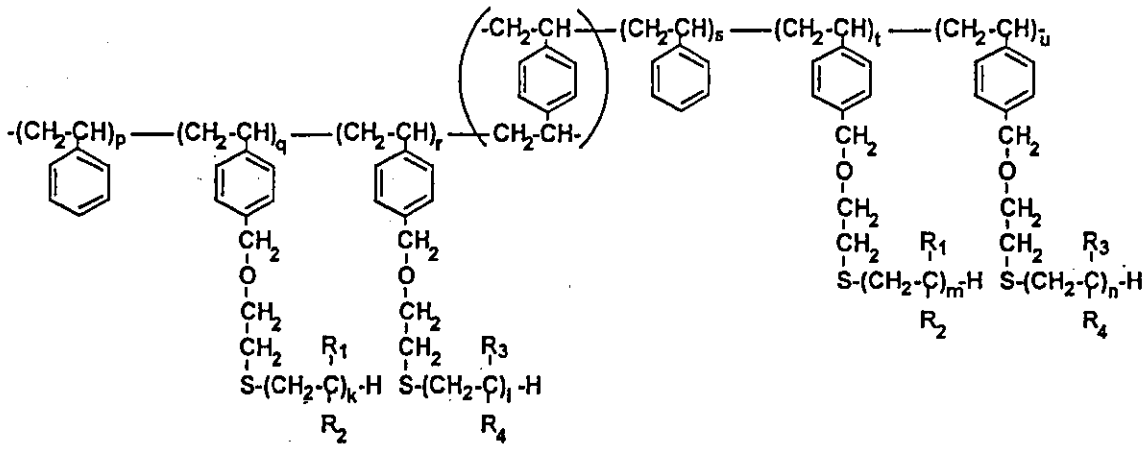

$R_{1,3}$	H, CH_3
$R_{2,4}$	$CONHCH(CH_3)_2$, $NHCOCH_3$, NH_2, COOH

$R_{1,3}$ is CH_3 only when $R_{2,4}$ is COOH.

Figure 1. Chemical structure of nanoparticles.

IR spectra confirmed that the resulting hydrophilic polyvinyl chains had been introduced to nanoparticles (data not shown). All nanoparticles were easily dispersible in water.

The effect of the crosslinking agent on the characteristics of PVAm nanoparticles was examined. As shown in Table 3, the zeta potential of nanoparticles without divinylbenzene (macromonomer: styrene = 1 : 10) was 13.8 mV at biological conditions (pH: 7.4; ionic strength: 0.15). This value increased to 22.1 mV when 1.5 mol% of divinylbenzene to styrene was added in the copolymerization. The zeta potential tended to decrease in inverse proportion to the amount of divinylbenzene although the nanoparticle size was independent of the amount of divinylbenzene. In the absence of divinylbenzene, nanoparticle size decreased and the zeta potential increased with increasing amounts of VAm macromonomers, consistent with results of our previous research.[19]

Enhancement of Human Calcitonin Oral Absorption by Nanoparticles

Plasma Concentration-Time Profile of Human Calcitonin

Figure 2 shows concentration-time profiles of hCT in plasma after subcutaneous administration of hCT saline

Table 3. Characteristics of PVAm nanoparticles.

Ratio of monomers			Particle size	Zeta potential
VAm macromonomer	Styrene	Divinylbenzene	(nm)	(mV)
1	40	0	645	11.1
1	5	0	296	16.2
1	10	0	533	13.8
1	10	0.15	296	22.1
1	10	0.3	1,431	21.9
1	10	0.45	273	19.7
1	10	0.6	1,202	17.7

MARCEL DEKKER, INC. • 270 MADISON AVENUE • NEW YORK, NY 10016

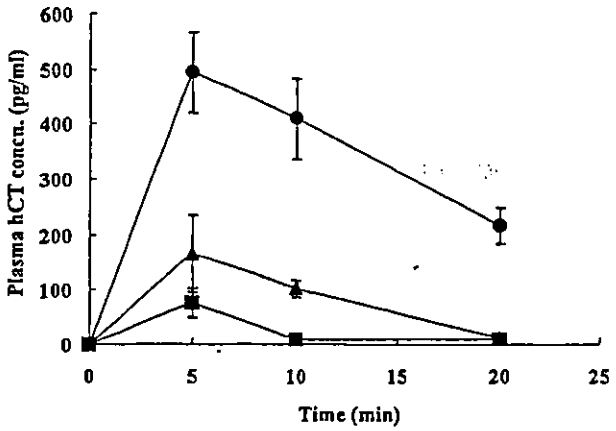

Figure 2. Concentration-time profiles of hCT. *Key:* ●, after subcutaneous administration of hCT saline solution (1 μg of hCT/2.5 mL/kg), ■, after oral administration of hCT aqueous solution (2.5 mg of hCT/2.5 mL/kg), and ▲, after oral administration of hCT with nanoparticles (0.25 mg of sCT with 25 mg of nanoparticles/2.5 mL/kg) in rats. A mixture of PVAm and PNIPAAm nanoparticles having a 1 : 40 molar ratio of macromonomers to styrene was used (5 mg of the respective nanoparticles/mL). Each value represents the mean ± SE of five experiments.

solution (1 μg/kg), after oral administration of hCT aqueous solution (2.5 mg/kg), and after oral administration of hCT with nanoparticles (0.25 mg/kg). A mixture of PVAm and PNIPAAm nanoparticles having a 1 : 40 molar ratio of macromonomers to styrene was used (5 mg of the respective nanoparticles/mL). After oral administration of hCT, the maximum blood concentration was reached in 5 min (t_{max}), irrespective of the presence of nanoparticles. The concentration of hCT in plasma subsequently decreased rapidly. T_{max} after subcutaneous administration of hCT was also 5 min and there was a linear decrease of hCT concentration.

Enhancement of Human Calcitonin Absorption by Nanoparticles

Figure 3 shows the relative bioavailability of hCT in the absence and the presence of nanoparticles having one kind of hydrophilic polymeric chains on their surfaces. The absorption rate of hCT after its oral administration without nanoparticles was 0.01%. This extremely low bioavailability was increased significantly when hCT was administered with nanoparticles. The absorption rate of hCT in the presence of cationic PVAm nanoparticles (VAm macromonomer : styrene = 1 : 40) was 0.16%, which was relatively higher than those rates in the presence of other nonionic and anionic nanoparticles, although differences between the four were not significant. This value increased to 0.28% after the oral administration of hCT with PVAm nanoparticles having an increased (1 : 5) molar ratio of the macromonomer to styrene. The absorption rate further increased to 0.66% when hCT was administered with PVAm nanoparticles whose polystyrene core was crosslinked by 1.5 mol% of divinylbenzene to styrene. This rate was significantly different from that after oral administration of hCT with PVAm nanoparticles (VAm macromonomer : styrene = 1 : 40). It decreased, however, with increased amounts of divinylbenzene.

Figure 4 shows the relative bioavailability of hCT in the presence of nanoparticles having two different kinds of hydrophilic polymeric chains on their surfaces, PVAm and either PNIPAAm or PMAA chains. The absorption rate of hCT was 0.20% after its oral administration with PVAm–PNIPAAm nanoparticles (VAm macromonomer : NIPAAm macromonomer : styrene = 1.5 : 0.5 : 80) and further decreased in proportion to the amount of the VAm macromonomer in the copolymerization. In contrast, the absorption rate of hCT exceeded 1.0% when the molar ratio of total macromonomers to styrene was increased to 1 : 5 in the preparation of PVAm–PNIPAAm nanoparticle (VAm macromonomer : NIPAAm macromonomer = 1.5 : 0.5). This absorption rate which was significantly different from that after oral administration of hCT with PVAm nanoparticles containing 1.5 mol% of divinylbenzene, however, decreased to 0.82% when hCT was administered with PVAm–PNIPAAm nanoparticles containing 3.0 mol% of divinylbenzene to styrene. The bioavailability of hCT in the presence of PVAm–PMAA nanoparticles (VAm macromonomer : MAA macromonomer : styrene = 1 : 1 : 10) was 0.48%, which was larger than that in the presence of PVAm nanoparticles (VAm macromonomer : styrene = 1 : 5) with an equal molar ratio of macromonomers to styrene. This value increased to 0.61% when hCT was administered with PVAm–PMAA nanoparticles containing 3.0 mol% of divinylbenzene to styrene although differences between the three were not significant.

DISCUSSION

Nanoparticles have been studied extensively as particulate carriers in several pharmaceutical and medical fields with much of this work focused on enhancing the absorption of peptide and protein drugs.[11,12,17] Couvreur and his co-workers showed that nanoparticles composed of polyalkylcyanoacrylate derivatives enhanced the absorption of orally administered insulin in

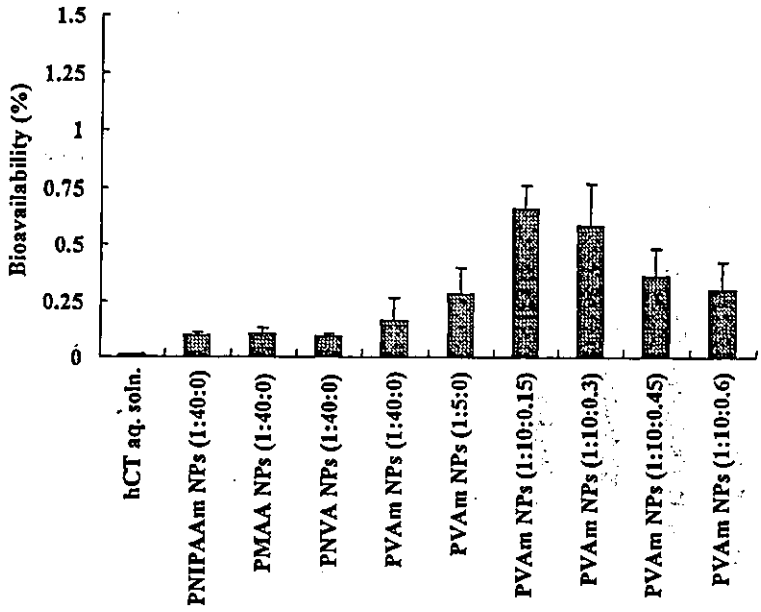

Figure 3. Relative bioavailability (%) after oral administration of hCT with or without nanoparticles having one kind of polymeric chains on their surfaces. The macromonomer : styrene : divinylbenzene molar ratio is given in parentheses. Each bar represents the mean ± SE of five experiments.

diabetic rats.[32,33] Kawashima et al. reported that the absorption of elcatonin, a modified eel calcitonin (eCT), via the GI tract of rats was improved by poly(*D, L*-lactide-glycolide) nanoparticles coated with the mucoadhesive cationic polymer, chitosan.[34] The absorption-enhancing function of chitosan was also reported by Lueßen et al.[35,36] The bioavailability of buserelin, which is an analogue of luteinizing hormone-releasing hormone, after its intraduodenum administration with hydrochloride salt of chitosan, increased by 5% to 5.1% (bioavailability of buserelin without any excipient: 0.1%). We developed nanoparticles having hydrophilic polymeric surface chains which can enhance the oral absorption of sCT.[13–19] In our series of studies, we showed that the enhancement of sCT absorption resulted mainly from the mucoadhesion of nanoparticles incorporating sCT in the intestinal tract and an increase in the stability of sCT against digestive enzymes. Furthermore, the effect of enhancing sCT absorption depended on the chemical structure of hydrophilic polymeric chains on the nanoparticle surface.[13–18] These findings led to the optimization of the chemical structure of nanoparticles showing the excellent enhancement effect of sCT absorption.[19]

The oral absorption of sCT was enhanced significantly by nanoparticles having PNIPAAm chains on their surfaces. However, that enhancement of hCT absorption was weaker than that by cationic PVAm nanoparticles (Fig. 3). It seems that this result was related to homology differences among the calcitonins (homology between sCT and hCT is about 50%). On the other hand, PVAm nanoparticles improved considerably the pharmacological effects of insulin and opioid peptide, compared with free drugs, which showed no efficacy when administered orally to rodents (data not published). These findings indicate that the optical chemical structure of nanoparticles varies according to characteristics of peptide drugs.

An increase in the amount of the VAm macromonomer in the PVAm nanoparticle preparations resulted in improved hCT absorption, and, furthermore, the addition of divinylbenzene improved hCT absorption, although the bioavailability decreased with increasing amounts of divinylbenzene (Fig. 3). The change in bioavailability corresponded to the change in the zeta potential. A relationship between bioavailability and nanoparticle size, however, was not found as well in our earlier study using sCT and PNIPAAm nanoparticles whose mean size was in the range of 400 nm to 800 nm.[13] As reported in our previous research,[19] the zeta potential of PVAm nanoparticles increased with increasing amounts of the VAm macromonomer. The maximum zeta potential of PVAm nanoparticles was obtained when 1.5 mol% of divinylbenzene to styrene was added in the copolymerization, as shown in Table 3. It is probable that the phase separation between a hydrophobic polystyrene core and hydrophilic PVAm

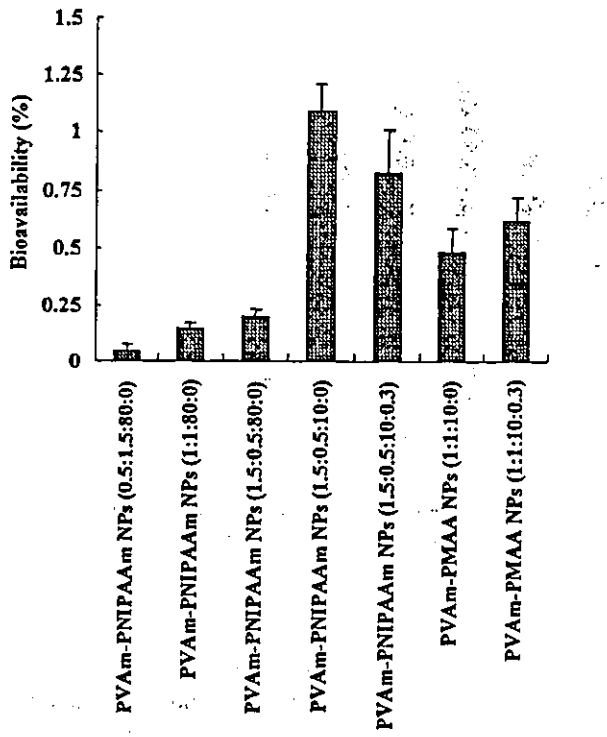

Figure 4. Relative bioavailability (%) after oral administration of hCT with nanoparticles having two different kinds of polymeric chains on their surfaces. The molar ratio of macromonomer-1 : macromonomer-2 : styrene : divinylbenzene is given in parentheses. The macromonomer-1 is VAm and the macromonomer-2 is NIPAAm or MAA. Each bar represents the mean ± SE of five experiments.

branches on the nanoparticle surface is facilitated by the formation of a more rigid polystyrene core through its crosslinking by divinylbenzene. Nevertheless, the zeta potential decreased with increasing amounts of divinylbenzene. This suggests that there is an optimal amount of the crosslinking agent for obtaining nanoparticles having a higher density of hydrophilic polymeric chains on their surfaces. The consistency between the bioavailability and the zeta potential indicates that the cationic moiety is indispensable for inducing a significant enhancement of hCT absorption.

Optimization of the chemical structure of nanoparticles for hCT was subsequently carried out by introducing PNIPAAm or PMAA chains onto the PVAm nanoparticle surface. PNVA chains were not used because our previous research suggested that they are able to eliminate the absorption-enhancing functions of PVAm nanoparticles by their shielding effect on the nanoparticle surface.[19] The enhancement effect of hCT absorption by PVAm–PNIPAAm nanoparticles was affected by the amount of PNIPAAm chains introduced onto the nanoparticle surface, whereby a small amount of PNIPAAm chains was most effective. The largest relative bioavailability obtained in this study (1.1%) was when VAm macromonomer, NIPAAm macromonomer, and styrene were copolymerized in the ratio of 1.5 : 0.5 : 10. This bioavailability, however, was decreased by the addition of divinylbenzene in the nanoparticle preparation, in contrast to the cases of simple PVAm nanoparticles and PVAm–PMAA nanoparticles which enhance hCT absorption as effectively as did PVAm nanoparticles. It is clear that the enhancement effect of hCT absorption by nanoparticles depends on the amount of divinylbenzene (Fig. 3). Three mol% of divinylbenzene to styrene may not be appropriate for forming the proper surface structure of PVAm–PNIPAAm nanoparticles (VAm macromonomer : NIPAAm macromonomer = 3 : 1) to enhance the hCT absorption efficiently. More detailed experiments are needed to explain the effect of crosslinking of the nanoparticle core on the absorption enhancement, including the surface analysis of nanoparticles.[17,23]

In research on polystyrene nanoparticles having surface hydrophilic polyvinyl chains, we showed that these nanoparticles are useful carriers to improve the bioavailability of poorly absorbed drugs such as peptides and proteins. Oral administration of hCT with PVAm–PNIPAAm nanoparticles (VAm macromonomer : NIPAAm macromonomer : styrene = 1.5 : 0.5 : 10) resulted in about 100-fold bioavailability. This effect matched that of chitosan hydrochloride for the absorption-enhancing function of peptide drugs.[35,36] However, the maximum improvement of hCT bioavailability by nanoparticles was slightly over 1%. It is considered that this enhancement effect of the oral absorption of calcitonin is unsatisfactory, although bisphosphonate, whose bioavailability is less than 1%, is used in the clinic as a drug for osteoporosis, which is the same indication as calcitonin.[37,38] Too fast a t_{max} implies the stabilizing effect of nanoparticles against hCT in the GI tract is insufficient. We will try to develop new types of nanoparticles which strongly prevent hCT from degrading in the GI tract, or to merge nanoparticle technology with other pharmaceutical technologies to acquire a superior oral enhancement effect for peptide and protein drugs.

CONCLUSIONS

The ability of nanoparticles having hydrophilic surface polymeric chains to enhance hCT absorption was examined in rats. The relative bioavailability of hCT without nanoparticles was 0.01%, but increased when hCT was administered with nanoparticles. Cationic PVAm nanoparticles

enhanced the hCT absorption more strongly compared to other nonionic and anionic nanoparticles. The absorption rate of hCT administered with PVAm nanoparticles increased in keeping with increased zeta potential of the nanoparticles. The bioavailability of hCT was 0.66% when it was given with PVAm nanoparticles (VAm macromonomer : styrene : divinylbenzene = 1 : 10 : 0.15) whose hydrophobic polystyrene core was crosslinked by divinylbenzene to facilitate the accumulation of the PVAm chains on the nanoparticle surface. These facts indicate that the cationic moiety is indispensable for inducing a significant enhancement of hCT absorption. We optimized the chemical structure of nanoparticles for hCT by introducing PNIPAAm or PMAA chains onto the PVAm nanoparticle surface. A maximum bioavailability of 1.1% was obtained after oral administeration of hCT with PVAm–PNIPAAm nanoparticles (VAm macromonomer : NIPAAm macromonomer : styrene = 1.5 : 0.5 : 10). The introduction of PMAA chains also contributed further improved enhancement effects of hCT absorption by PVAm nanoparticles.

ACKNOWLEDGMENTS

This work was financially supported in part by a grant-in-aid for scientific research (No. 11480259 and 10555326) from the Ministry of Education, Science, Sports and Culture of Japan. The authors express their appreciation to Dr. Masahiro Hayashi of Tokyo University, Pharmacy and Life Science, for fruitful discussion on the mechanism of hCT absorption in the presence of nanoparticles.

REFERENCES

1. Van Hoogdalem, E.J.; De Boer, A.G.; Breimer, D.D. Intestinal drug absorption enhancement: an overview. Pharmac. Ther. **1989**, *44*, 407–443.
2. Lee, V.H.L.; Yamamoto, A. Penetration and enzymatic barriers to peptide and protein absorption. Adv. Drug Deliv. Rev. **1990**, *4*, 171–207.
3. Yamamoto, A.; Muranishi, S. Rectal drug delivery systems: improvement of rectal peptide absorption by absorption enhancers, protease inhibitors and chemical modification. Adv. Drug Deliv. Rev. **1997**, *28*, 275–299.
4. Harris, A.S. Clinical opportunities provided by the nasal administration of peptides. Drug Targeting **1993**, *1*, 101–116.
5. Fujita, T.; Fujita, T.; Morikawa, K.; Tanaka, H.; Iemura, O.; Yamamoto, A.; Muranishi, S. Improvement of intestinal absorption of human calcitonin by chemical modification with fatty acid: synergistic effects of acylation and absorption enhancers. Int. J. Pharm. **1996**, *134*, 47–57.
6. Lee, V.H.L. Protease inhibitors and penetration enhancers as approaches to modify peptide absorption. J. Control. Rel. **1990**, *13*, 213–233.
7. Saffran, M.; Kumar, G.S.; Savariar, C.; Burnham, J.C.; Williams, F.; Neckers, D.C. A new approach to the oral administration of insulin and other peptide drugs. Science **1986**, *233*, 1081–1084.
8. Sakuma, S.; Lu, Z.R.; Kopečková, P.; Kopeček, J. Biorecognizable HPMA copolymer-drug conjugates for colon-specific delivery of 9-aminocamptothecin. J. Control. Rel. **2001**, *75*, 365–379.
9. Gu, J.P.; Robinson, J.R.; Leung, S.H.S. Binding of acrylic polymers to mucin/epithelial surfaces: structure-property relationships. Crit. Rev. Ther. Drug Carrier Syst. **1988**, *5*, 21–67.
10. Takeuchi, H.; Yamamoto, H.; Kawashima, Y. Mucoadhesive nanoparticulate systems for peptide drug delivery. Adv. Drug Deliv. Rev. **2001**, *47*, 39–37.
11. Kreuter, J. Peroral administration of nanoparticles. Adv. Drug Deliv. Rev. **1991**, *7*, 71–86.
12. Couvreur, P.; Puisieux, F. Nano- and microparticles for the delivery of polypeptides and proteins. Adv. Drug Deliv. Rev. **1993**, *10*, 141–162.
13. Sakuma, S.; Suzuki, N.; Kikuchi, H.; Hiwatari, K.; Arikawa, K.; Kishida, A.; Akashi, M. Oral peptide delivery using nanoparticles composed of novel graft copolymers having hydrophobic backbone and hydrophilic branches. Int. J. Pharm. **1997**, *149*, 93–106.
14. Sakuma, S.; Suzuki, N.; Kikuchi, H.; Hiwatari, K.; Arikawa, K.; Kishida, A.; Akashi, M. Absorption enhancement of orally administered salmon calcitonin by polystyrene nanoparticles having poly(N-isopropylacrylamide) branches on their surfaces. Int. J. Pharm. **1997**, *158*, 69–78.
15. Sakuma, S.; Ishida, Y.; Sudo, R.; Suzuki, N.; Kikuchi, H.; Hiwatari, K.; Kishida, A.; Akashi, M.; Hayashi, M. Stabilization of salmon calcitonin by polystyrene nanoparticles having surface hydrophilic polymeric chains, against enzymatic degradation. Int. J. Pharm. **1997**, *159*, 181–189.
16. Sakuma, S.; Sudo, R.; Suzuki, N.; Kikuchi, H.; Hiwatari, K.; Akashi, M.; Hayashi, M. Mucoadhesion of polystyrene nanoparticles having surface hydrophilic polymeric chains in the gastrointestinal tract. Int. J. Pharm. **1999**, *177*, 161–172.
17. Sakuma, S.; Hayashi, M.; Akashi, M. Design of nanoparticles composed of graft copolymers for oral peptide delivery. Adv. Drug Deliv. Rev. **2001**, *47*, 21–37.
18. Sakuma, S.; Sudo, R.; Suzuki, N.; Kikuchi, H.; Akashi, M.; Ishida, Y.; Hayashi, M. Behavior of mucoadhesive nanoparticles having hydrophilic

polymeric chains in the intestinal membrane. J. Control. Rel. **2002**, *81*, 282–290.
19. Sakuma, S.; Suzuki, N.; Sudo, R.; Hiwatari, K.; Kishida, A.; Akashi, M. Optimized chemical structure of nanoparticles as carriers for oral delivery of salmon calcitonin. Int. J. Pharm. **2002**, *239*, 185–195.
20. Akashi, M.; Kirikihara, I.; Miyauchi, N. Synthesis and polymerization of a styryl terminated oligovinylpyrrolidone macromonomer. Angew. Macromol. Chem. **1985**, *132*, 81–89.
21. Akashi, M.; Wada, M.; Yanase, S.; Miyauchi, N. Polymer drugs and polymeric srugs. II. Synthesis of water dispersible microspheres having 5-fluorouracil and theophylline using a water soluble macromonomer. J. Polym. Sci. Polym. Lett. **1989**, *27*, 377–380.
22. Akashi, M.; Chao, D.; Yashima, E.; Miyauchi, N. Graft copolymers having hydrophobic backbone and hydrophilic branches, V. Microspheres obtained by the copolymerization of poly(ethylene glycol) macromonomer with methyl methacrylate. J. Appl. Polym. Sci. **1990**, *39*, 2027–2030.
23. Akashi, M.; Yanagi, T.; Yashima, E.; Miyauchi, N. Graft copolymers having hydrophobic backbone and hydrophilic branches IV. A copolymerization study of water-soluble oligovinylpyrrolidone macromonomers. J. Polym. Sci. Polym. Chem. **1989**, *27*, 3521–3530.
24. Capek, I.; Akashi, M. On the kinetics of free radical polymerization of macromonomers. J. Macromol. Sci.-Rev. Macromol. Chem. Phys. **1993**, *C33*, 369–436.
25. Yabuta, M.; Suzuki, Y.; Ohsuye, K. High expression of a recombinant human calcitonin precursor peptide in escherichia coli. Appl. Microbiol. Biotechnol. **1995**, *42*, 703–708.
26. Furukawa, K.; Okuno, K.; Onai, S.; Sugimura, K.; Yoko-o, Y.; Ishibashi, Y.; Oshima, Y.; Tsuruoka, N.; Tanaka, S.; Ohsuye, K. Production of an α-amidating enzyme (α-AE) in recombinant CHO cells. In Animal Cell Technology: Basic & Applied Aspects; Kaminogawa, S., et al. Eds.; Kluwer Academic Publishers, 1993; Vol. 5, 493–499.
27. Riza, M.; Tokura, S.; Kishida, A.; Akashi, M. Graft copolymers having a hydrophobic backbone and hydrophilic branches. IX. Preparation of water-dispersible microspheres having polycationic branches on their surfaces. N. Polym. Mater. **1994**, *4*, 189–198.
28. Riza, M.; Tokura, S.; Iwasaki, M.; Yashima, E.; Kishida, A.; Akashi, M. Graft copolymers having hydrophobic backbone and hydrophilic branches. X. Preparation and properties of water-dispersible polyanionic microspheres having poly(methacrylic acid) branches on their surfaces. J. Polym. Sci. Polym. Chem. **1995**, *33*, 1219–1225.
29. Chen, M.Q.; Kishida, A.; Akashi, M. Graft copolymers having hydrophobic backbone and hydrophilic branches. XI. Preparation and thermosensitive properties of polystyrene microspheres having poly(N-isopropylacrylamide) branches on their surfaces. J. Polym. Sci. Polym. Chem. **1996**, *34*, 2213–2220.
30. Chen, M.Q.; Serizawa, T.; Akashi, M. Graft copolymers having hydrophobic backbone and hydrophilic branches. Polystyrene microspheres with poly(N-isopropylacrylamide) branches on their surfaces: size control factors and thermosensitive behavior. Polym. Adv. Tech. **1999**, *10*, 120–126.
31. Miyauchi, Y.; Vaitukaitis, J.L.; Nieschlag, E.; Lipset, M.B. Enzymatic radioiodination of gonadotropins. J. Clin. Endocrinol. Metab. **1972**, *34*, 23–28.
32. Damgé, C.; Michel, C.; Aprahamian, M.; Couvreur, P. New approach for oral administration of insulin with polyalkylcyanoacrylate nanocapsules as drug carriers. Diabetes **1988**, *37*, 246–251.
33. Damgé, C.; Michel, C.; Aprahamian, M.; Couvreur, P.; Devissaguet, J.P. Nanoparticles as carriers for oral peptide delivery. J. Control. Rel. **1990**, *13*, 233–239.
34. Kawashima, Y.; Yamamoto, H.; Takeuchi, H.; Kuno, Y. Mucoadhesive DL-lactide/glycolide copolymer nanospheres coated with chitosan to improve oral delivery of calcitonin. Pharm. Develop. and Technol. **2000**, *5*, 77–85.
35. Lueßen, H.L.; de Leeuw, B.J.; Langemeyer, M.W.E.; de Boer, A.G.; Verhoef, J.C.; Junginger, H.E. Mucoadhesive polymers in peroral peptide drug delivery. VI. Carbomer and chitosan improve the intestinal absorption of the peptide drug buserelin in vivo. Pharm. Res. **1996**, *13*, 1668–1672.
36. Bernkop-Schnurch, A. Chitosan and its derivatives: potential excipients for peroral peptide delivery systems. Int. J. Pharm. **2000**, *194*, 1–13.
37. Major, P.P.; Lipton, A.; Berenson, J.; Hortobagyi, G. Oral bisphosphonates: a review of clinical use in patients with bone metastases. Cancer **2000**, *88*, 6–14.
38. Hoffman, A.; Stepensky, D.; Ezra, A.; Van Gelder, J.M.; Golomb, G. Mode of administration-dependent pharmacokinetics of bisphosphonates and bioavailability determination. Int. J. Pharm. **2001**, *220*, 1–11.

Received September 10, 2002
Accepted October 27, 2002

Hydroxyapatite and bFGF Coating of Detachable Coils for Endovascular Occlusion of Experimental Aneurysm

T. SHIMOZURU, T. KAMEZAWA, J. KURATSU, N. SAKAI*, I. NAGATA*, A. KISHIDA**, M. AKASHI***, M. MATSUSAKI***

Department of Neurosurgery, Faculty of Medicine, Kagoshima University;
** Department of Neurosurgery, National Cardio-Vascular Center;*
*** Department of Bioengineering, National Cardio-Vascular Center Research Institute;*
**** Department of Applied Chemistry and Chemical Engineering, Faculty of Engineering, Kagoshima University*

Key words: experimental aneurysm, embolization, hydroxyapatite, bFGF

Summary

The purpose of this study was to evaluate the effect of hydroxyapatite (HAp) and fibroblast growth factor-basic (bFGF) coating on Guglielmi detachable coils (GDCs) in an experimental aneurysm model. A total of 18 aneurysms were experimentally made in the common carotid arteries of swine. Embolization was done on these aneurysms using standard GDCs and coated GDCs with HAp (GDC-HAp) and with bFGF (GDC-HAp-bFGF). The animals were then killed 14 days after embolization. The development of tissue scarring and coverage the aneurysm's orifice were evaluated macroscopically. No significant difference of volume ratio of the coils exited in each groups. Macroscopically, covering ratio of fibrous membrane at the neck of aneurysms were 88.3 ± 14.7% in a group with GDC-HAp-bFGF, while it were 26.7 ± 15.3% in a group with standard GDC and it was 41.7 ± 31.7% in a group with GDC-HAp. These results indicated that coating by hydroxyapatite and bFGF might facilitate a wound healing in an experimental aneurysm model.

Introduction

Several studies dealing with long-term angiographic and histopathologic examinations showed that the treated aneurysms developed coil compaction and recanalization and coverage across the neck of the aneurysm was not recognized [1-3,7]. In our previous study, coils coated by HAp might enhance intra-aneurysmal scar formation and re-endothelialization across the neck of aneurysm [10].

Platinum coils were inert and not cell-adhesive. Hydroxyapatite is a biological carrier with enhancement of thrombus organization, and basic FGF is a potent mitogenic agent for wide variety of mesoderm -drived cells including fibroblast, capillary and endocardial endotherial cells, smooth muscle cells. Apatite formation on/in hydrogel matrices were developed using a novel alternate soaking process [12]. This study was designed to check the hypothesis that embolization with coating coils developes endotherialization across the neck in an experimental intracerebral aneurysm model of swine.

Material and Methods

1) Coil Coating

GDC, sizes 18 (6-20 cm length, 3-8 mm helix diameter, platinum coil with 0.015 inches thickness; Boston Scientific Corp., Fremont, CA) was used for embolization. Hydroxyapatite coating method was reported previously. The GDC-HAp were immersed in a solution con-

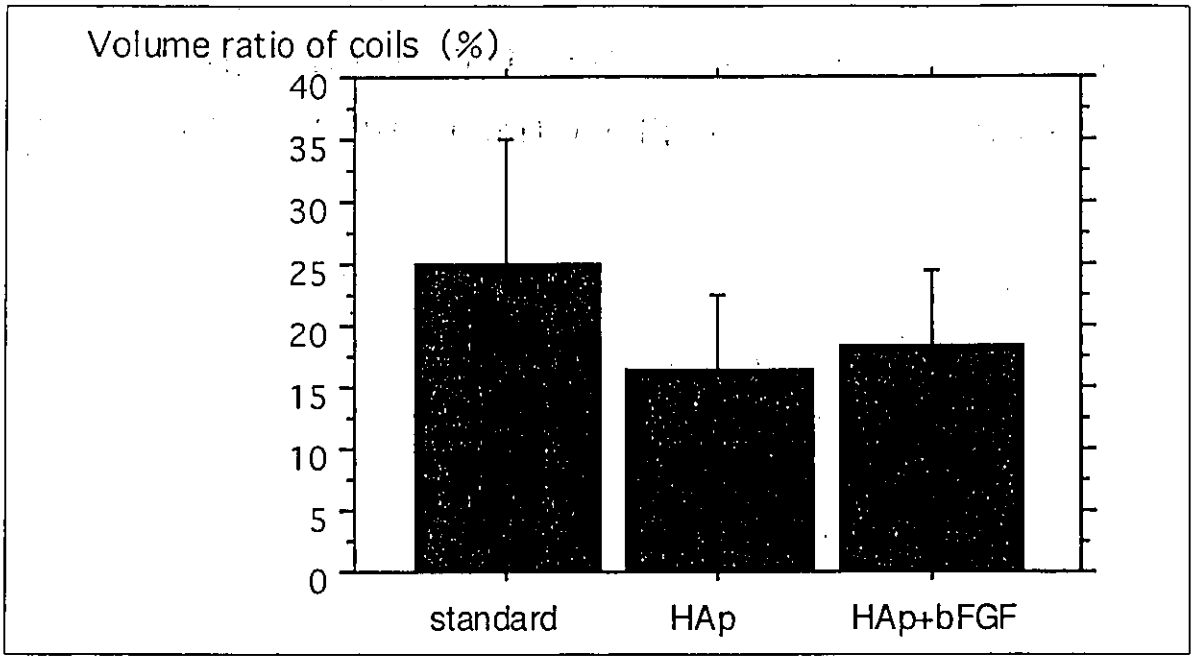

Figure 1 Volume ratio of coils in each groups.

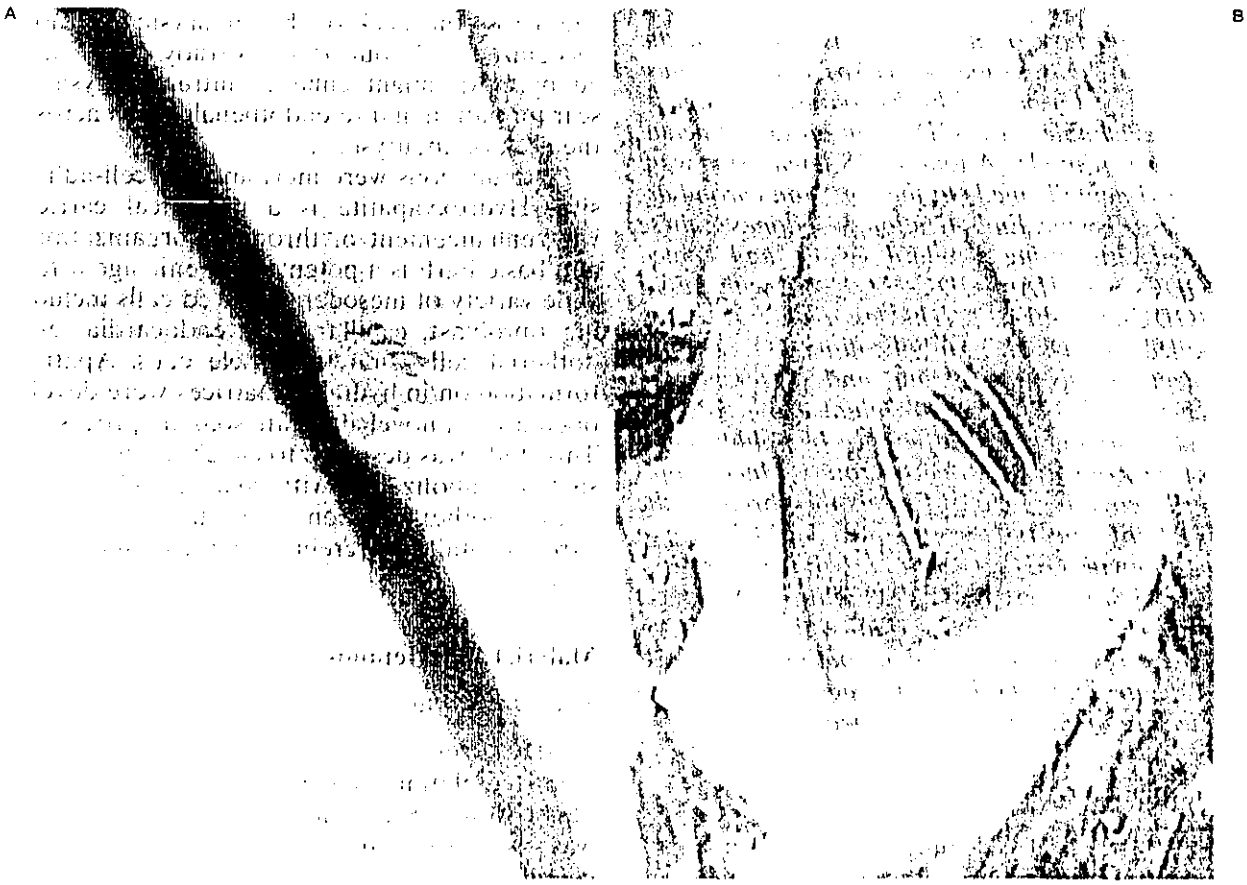

Figure 2 A) Angiograms of experimental aneurysms embolized by GDC-HAp. After tight packing of aneurysms, complete occlusion was recognized 2 weeks later. B) Macroscopic appearances of an aneurysmal orifice. The orifice of aneurysm was covered partially with fibrous tissue.

Figure 3 A) Angiograms of experimental aneurysms embolized by GDC-HAp-bFGF. Complete occlusion was recognized 2 weeks later. B) Macroscopic appearances of an aneurysmal orifice. The orifice of aneurysm was covered completely with thick fibrous tissue.

taining 1μg/ml recombinant human bFGF (Sigma Corp, St. Louis, USA) during 20 minutes before embolization.

2) Aneurysm Construction and Coil Embolization

The details of aneurysm construction and coil embolizationhave been reported [10]. A total of 18 saccular aneurysms with 5 mm in neck and 6 to 8 mm in length were experimentally made in bilateral common carotid arteries of nine swine using a microsurgical technique. GDCs, were placed in the lumen of the aneurysm until noadditional coils could fit into the aneurysm.

3) Final Angiographic and Histopathologic Studies

Final angiography was performed before killing animals to document the radioanatomical results. Then the aneurysm-parent artery complex was removed and parent artery of the specimens were cut from the bottom to the orifice and direct view of aneurysm orifice and coil surface was obtained and photographically documented.

Results

1) Angiographical Studies

Embolization was performed for 18 aneurysms.

Fourteen days after embolization, three aneurysms had parent artery occlusion and thrombus formation from orifice to parent artery. Angiographic examination in 15 aneurysms were done. Two of three aneurysms embolized by standard GDCs and five of six aneurysms used by GDC-HAp and all GDC-HAp-bFGF demonstrated neally total occlusion (figures 2,3). One standard GDC and one

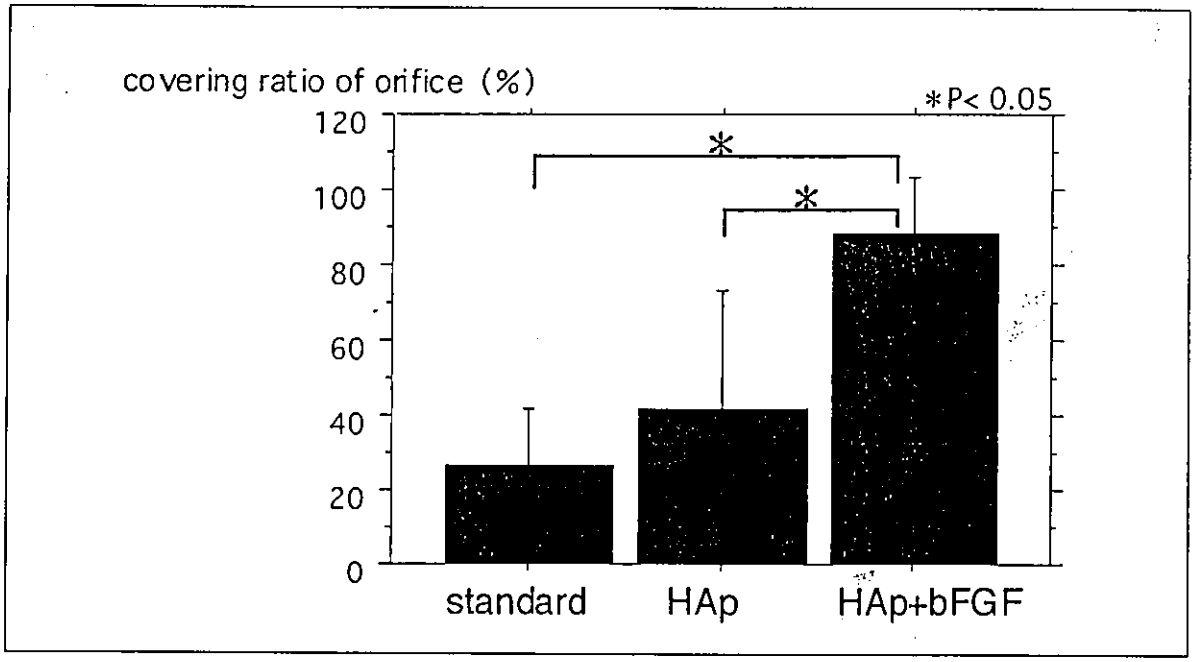

Figure 4 Covering ratio of orifice of aneurysms in each groups.

GDC-HAp of these aneurysms showed recanalization.

Total length of coils used in each aneurysm were from 28 cm to 72 cm (mean, 51.2 ± 6.2 cm), volume ratio of coils with respect to aneurysmal volume were approximately 18.5% to 25%. Significant difference of volume ratio of the coils in each groups was not recognized (figure 1).

Volume ratio of coils; Length of coils x (coil radius) 2 x π /sac volume

2) Macroscopic Findings

Macroscopic examinations of the aneurysms showed significant differences between the standard GDC and GDC-HAp-bFGFs. The surface of the standard GDCs was covered with a thin fibrin-like white material. On the other hand, a denser and thicker fibrous tissue was observed at the neck of aneurysms embolized with GDC-HAp-bFGFs (figures 2,3). The predominantly fibrous scarring was covered with neoendothelium arising from the edges of the neck of the aneurysm. Covering of fibrous membrane in the orifice was 26.7% of the aneurysms embolized by standard GDCs, 41.7 ± 31.7% of those by GDC-HAps, 88.3 ± 14.7% of those by GDC-HAp-bFGF (figure 4). There was statistically significant difference ($P < 0.05$) between standard GDCs and GDC-HAp-bFGF.

Discussion

We found that embolization with GDC coated by HAp and bFGF stimulate the healing process of lateral wall aneurysm of swine model. Fibrous menbrane covering of neck were recognized in GDC coated by HAp and bFGF, compared with of standard GDCs.

Several studies have stated that important anatomic limitations on complete occlusion associated with this endovascular therapeutic procedure[1,6,13]. Platinum is inert biologically and does not elicit a significant biological response on its surface. Coating on platinum with proteins might be difficult, by polyester fiber[4] collagen cores[2], incorporating collagen thread[11], ion implantation with fibronectin, laminin[8] to modify coil thrombogenicity and inflammatory cellular response.

In this study, we used GDCs coated by HAp whitch enhance thrombogenecity and bFGF whitch promote neointimal hyperplasia in the healing process of aneurysm.

There are several limitations in our study. Lateral side wall aneurysm in the swine has a strong tendency for spontaneous wound healing. Owing to apprehension of the exess thrombogenecity of HAp, we performed strict heparinization and anti-platelet drugs similar to clinical procedure[10]. Three of 18 aneurysms em-

bolized had parent artery occlusion. Thrombogenecity play an important role in the first stage of wound healing and then ECM and basicc Fibroblast growth factor (bFGF) play same role in second stage[7,14].

Some studies have examined the effect of various proteins on SMC proliferation, attachment, and the growth of endothelial cells derived from artery wall[13]. In second limitation, We used infiltration of GDC-HAp into a solution containing 1μg/ml bFGF. But, activity of bFGF is very short. We reported histologic changes in aneurysms embolized with GDCs-HAp in the early stage[10]. Coating of surfice GDC-HAp using other proteins such as bonding with bFGF, may be of value in late stage of complete aneurismal occlusion.

Conclusions

GDCs coated by HAp and bFGF show a faster neoendothelial proliferation in the aneurysm neck.

Such promoted biological response may decrease the chances of coil compaction and recanalization in human cerebral aneurysms treated by GDCs.

Acknowledgements

The authors acknowledge the technical assistance of R.Uemura, H. Kanesugi, K. Kawaguchi, K. Kori, N. Komaki, Technical Research Center of Boston Scientific Co., Miyazaki, Japan.

References

1 Bavinzski G, Talazoglu V et Al: Gross and microscopic histopathological findings in aneurysms of the human brain treated with Guglielmi detachable coils. J Neurosurg 91 (2): 284-293, 1999.
2 Dawson RC, Krisht AF et Al: Treatment of experimental aneurysms using collagen-coated microcoils. Neurosurgery 36 (1): 133-139, discussion 139-140, 1995.
3 Gruber A, Killer M et Al: Clinical and angiographic results of endosaccular coiling treatment of giant and very large intracranial aneurysms: a 7-year, single-center experience. Neurosurgery 45 (4): 793-803, discussion 803-794, 1999.
4 Kallmes DF, Helm GA et Al: Histologic evaluation of platinum coil embolization in an aneurysm model in rabbits. Radiology 213 (1): 217-222, 1999.
5 Kwan ES, Heilman CB et Al: Endovascular packing of carotid bifurcation aneurysm with polyester fiber-coated platinum coils in a rabbit model. Am J Neuroradiol 14 (2): 323-333, 1993.
6 Malisch TW, Guglielmi G et Al: Intracranial aneurysms treated with the Guglielmi detachable coil: midterm clinical results in a consecutive series of 100 patients. J Neurosurg 87 (2): 176-183, 1997.
7 Mawad ME, Mawad JK et Al: Long-term histopathologic changes in canine aneurysms embolized with Guglielmi detachable coils. Am J Neuroradiol 16 (1): 7-13, 1995.
8 Murayama Y, Vinuela F et Al: Ion implantation and protein coating of detachable coils for endovascular treatment of cerebral aneurysms: concepts and preliminary results in swine models. Neurosurgery 40 (6): 1233-1243, discussion 1243-1234, 1997.
9 Raymond J, Venne D et Al: Healing mechanisms in experimental aneurysms. I. Vascular smooth muscle cells and neointima formation. J Neuroradiol 26 (1): 7-20, 1999.
10 Shimozuru T, Kuratsu J et Al: Hydroxyapatite coating of detachable coils for endovascular occlusion of experimental aneurysms. Interventional neuroradiology 7 (suppl 1): 105-110, 2001.
11 Szikora I, Wakhloo AK et Al: Initial experience with collagen-filled Guglielmi detachable coils for endovascular treatment of experimental aneurysms. Am J Neuroradiol 18 (4): 667-672, 1997.
12 Taguchi T, Muraoka Y et Al: Apatite coating on hydrophilic polymer-grafted poly(ethylene) films using an alternate soaking process. Biomaterials 22 (1): 53-58, 2001.
13 Tamatani S, Ozawa T et Al: Histological interaction of cultured endothelial cells and endovascular embolic materials coated with extracellular matrix. J Neurosurg 86 (1): 109-112, 1997.
14 Venne D, Raymond J et Al: Healing of experimental aneurysms. II: Platelet extracts can increase the thickness of the neointima at the neck of treated aneurysms. J Neuroradiol 26 (2): 92-100, 1999.

T. Shimozuru, M.D.
Department of Neurosurgery
Faculty of Medicine
Kagoshima University
Japan

6th Meeting of the Asian - Australasian Federation of Interventional and Therapeutic Neuroradiology

March 25th - 27th, 2004
Bangkok, Thailand

1st Announcement

President
Suthisak Suthiponchai, M.D.

Invited Speakers
Pierre Lasjaunias, M.D. Ph.D. (Paris, France). In Sup Choi, M.D. (Burlington, USA), Jaques Dion, M.D., FRCP (Atlanta, USA), Karel terBrugge M.D., FRCP (Toronto, Canada), Georges Rodesch, M.D. (Paris, France) etc.

TOPICS

- Neurosciences in vascular diseases
- Functional neuro-anatomy
- Recent advances in stroke management
- Vascular proliferations and angiogenesis
- Recent advances in neurovascular imaging
- Spine and spinal cord vascular diseases
- Cerebral AVMs / dural AVMs
- Cerebral aneurysms
- Neurovascular trauma
- Stereotactic radiosurgery in neurovascular disease
- New technology and devices in endovascular treatment

Congress Secretariat

Anchalee Churojana, M.D.
Department of Radiology, Siriraj Hospital, Mahidol University
2 Prannok Rd., Bangkoknoi, Bangkok Thailand 10400
Tel: +662 419 7086 - Fax: +662 412 7785
Web site: www.aafitn.org - E-mail: office@aafitn.org

JOURNAL OF MATERIALS SCIENCE: MATERIALS IN MEDICINE 14 (2003) 1–5

Nano-scaled hydroxyapatite/polymer composite I. Coating of sintered hydroxyapatite particles on poly(γ-methacryloxypropyl trimethoxysilane)-grafted silk fibroin fibers through chemical bonding

T. FURUZONO*, A. KISHIDA
Department of Bioengineering, National Cardiovascular Center Research Institute, 5-7-1 Fujishiro-dai, Suita, Osaka 565-8565, Japan
E-mail: furuzono@ri.ncvc.go.jp

J. TANAKA
Biomaterials Center, Independent Administrative Institution, National Institute for Materials Science, 1-1 Namiki, Tsukuba, Ibaraki 305-0044, Japan

The inorganic–organic composite consisting of nano-scaled hydroxyapatite (HAp) and silk fibroin (SF) fibers was prepared through covalent linkage to develop a novel biomaterial for a soft-tissue-compatible material. The preparation of the composite was conducted through the three-step procedure consisting of chemical modification using 2-methacryloxyethyl isocyanate (MOI) monomer to introduce vinyl groups on SF, poly(γ-methacryloxypropyl trimethoxysilane) (MPTS) graft-polymerization on SF, and coupling process between the surface of polyMPTS-grafted SF and HAp nano-particles. The amount of the graft-polymerization of polyMPTS through vinyl groups was well controlled by the reaction time. The nano-crystals were subsequently coated on the grafted fibers by heating at 120 °C for 2 h in a vacuum. The crystalline structure of the SF substrate did not change in the procedure. In the SEM observation of the composite surface, it was found that the bonded nano-crystals were separated and partially aggregated with several crystals attached on the SF fiber surface. The HAp particles adhered more strongly on the SF surface with separation or aggregation of several crystals than on the surface of the original SF after ultrasonic treatment.

1. Introduction

Hydroxyapatite (HAp) has unique properties for biomaterials such as hard-tissue-compatible material for bone and tooth [1] and also soft-tissue-compatible material for skin tissue [2]. From the point of view of soft-tissue-compatible material made up of HAp, although the reasons for the compatibility have not been manifested completely, one of them might be favorable to adsorption of adhesion molecules or growth factors *in vivo* on the HAp surface [3]. Aoki *et al.* first developed a percutaneous device clinically using a ceramic disk made of HAp in catheters, blood pressure transducers, leads, and electrodes [2]. A rigid ceramic disk that partially protrudes through the skin, however, limits a patient's mobility and causes discomfort [4]. The hard and brittle nature of HAp limits the development of a percutaneous device. To overcome this problem, a novel inorganic–organic composite consisting of micro- or nano-scaled HAp particles and polymer substrate via a covalent linkage has been designed.

An unique composite of sintered HAp micro-particles covalently coupled to a silicone elastomer as soft-tissue-compatible material was developed recently [5, 6]. The HAp particles were attached to the silicone substrate covalently without damaging the mechanical properties of the polymer substrate. In this way, the adhesion strength between the HAp particle and polymer substrate, however, was believed to be unsatisfactory because a commercial grade of a HAp spherical particle with an average diameter of 2.0 μm was used. To increase the interaction between the HAp particle and substrate surface, a nano-scaled HAp particle with a larger surface-area of adhesion on a polymer substrate has been developed by an emulsion system [7, 8]. It is expected

*Author to whom all correspondence should be addressed. Present address: Japan Science and Technology corporation (JST), Kawaguchi Center Building 1-8, Honcho 4-chome, Kawaguchi, Saitama 332-0012, Japan.

0957–4530

that the inorganic–organic composite can be satisfactorily developed using the nano-scaled HAp particles.

In this report, we develop a novel composite consisting of a nano-scaled HAp particle and a silk fibroin (SF) fiber as a polymer substrate through covalent linkage. The SF fiber shows good qualities for implant materials, such as good mechanical properties, moldability, possessing many functional groups on the surface, and actual results as a suture in the medical field for a long period. However, there is a drawback, for SF sometimes causes inflammation in a living body. If HAp is coated on SF, the inflammation is expected to be reduced compared with the original SF. We selected SF as a polymer substrate to develop a composite with HAp since the SF fiber can add mechanical strength and flexibility to the inorganic material. The chemical modification of the HAp surface in advance is not necessary for the preparation of the composite.

2. Materials and methods

2.1. Materials

For the preparation of the nano-scaled HAp, calcium hydroxide [$Ca(OH)_2$], potassium dihydrogen phosphate (KH_2PO_4), dedecane as a continuous oil phase, and pentaethylene glycol dodecyl ether as a nonionic surfactant were purchased from Wako Pure Chemical Industries, Ltd. (Osaka, Japan). Dimethyl sulfoxide (DMSO) and ethanol as solvents, di-n-butyltin (IV) dilaurate as a catalyst, and hydroquinone as a polymerization inhibitor were also purchased from the same chemical company. Degummed habutae fabric (Fujimura-Seishi Co., Kochi, Japan), which is the variety name, made of silk from *Bomboyx mori* was cleaned by soxhlet extractor with acetone for 24 h to remove the wax, rinsed with distilled water, and freeze-dried for 24 h. 2-methacryloxyethyl isocyanate (MOI) and γ-methacryloxypropyl trimethoxysilane (MPTS) monomers were donated by Showa Denko Co. (Tokyo, Japan) and Shin-Etsu Chemical Industries Co. (Tokyo, Japan), respectively (Scheme 1).

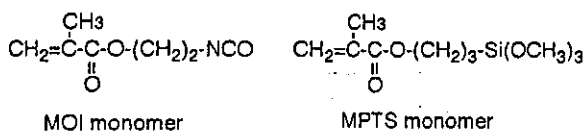

Scheme 1 Chemical structures of MOI and MPTS monomers.

2.2. Measurements

An attenuated total reflection (ATR) and diffuse reflectance Fourier transform infrared spectrometry (FT-IR) was recorded using a Spectrum One (Perkin-Elmer Inc., MA, USA). The resolution of each spectrum was 4 cm^{-1} with 16 s scan times ranging from 4000 to 400 cm^{-1}. The HAp and the composite were observed with a scanning electron microscope (SEM, JSM-6301F, Jeol Ltd., Tokyo, Japan). X-ray diffraction measurements were conducted at 2θ (varying from 2° to 75°) using an automatic diffractometer (RAD-X, Rigaku Inter-national Co., Tokyo, Japan) with CuKα radiation (λ = 0.154 nm) and an Ni filter generated at 45 kV and 25 mA. Data were collected using a receiving slit of 0.15 mm, 2θ scanning at 2°/min, and a 2θ-scan step of 0.02°.

2.3. Sample preparation

Nano-particles of HAp were prepared by the emulsion system described in the former reports [7, 8]. Briefly, 10 cm^3 of an aqueous suspension of 2.5 mol dm^{-3} of $Ca(OH)_2$ was poured into 40 cm^3 of the dodecane containing 0.5 g of the surfactant. After rapidly stirring the W/O emulsion, 10 cm^3 of 1.5 mol dm^{-3} KH_2PO_4 aqueous solution was added into the system, and reacted at 50 °C for 24 h. After purification by centrifugation with ethanol and water, the powder was calcined at 800 °C for 1 h at a 10 °C/min heating rate. Finally, truncated rod-shaped HAp particles below 200 nm in length were obtained. Fig. 1 shows the HAp particles by SEM observation. These particles possess a large surface area with an a-plane and show a slight calcium deficiency (Ca/P = 1.61) containing carbonate [7].

Before the graft-polymerization of polyMPTS, an MOI monomer was reacted on the SF due to the donation of vinyl bonds according to the former literature [9]. The SF fabrics, 1.8 cm in diameter, were used in this reaction. The MOI-modified SF with 7.0–8.0 wt % of weight gain was used in the graft-polymerization of polyMPTS. MPTS grafted via the vinyl double bond of MOI was reacted on the SF using AIBN as an initiator. 2.0 mmol of the MPTS monomer and 0.4 mmol of AIBN were dissolved in 5.0 cm^3 of DMSO. Six pieces of the SF were immersed in the reaction solution in 50 cm^3 thick-walled polymerization tubes. The tubes were degassed by freezing and evacuating four times and sealed. Graft-polymerization was conducted at 60 °C for different periods. PolyMPTS-grafted fabrics were collected from the reaction system, washed with DMSO and methanol, and finally dried by vacuum for 24 h at room temperature. Weight gain was calculated from the increase in weight of the dried MOI-modified SF after graft-polymerization with MPTS as follows;

$$\text{weight gain (wt \%)} = (W_2 - W_1)/W_1 \times 100$$

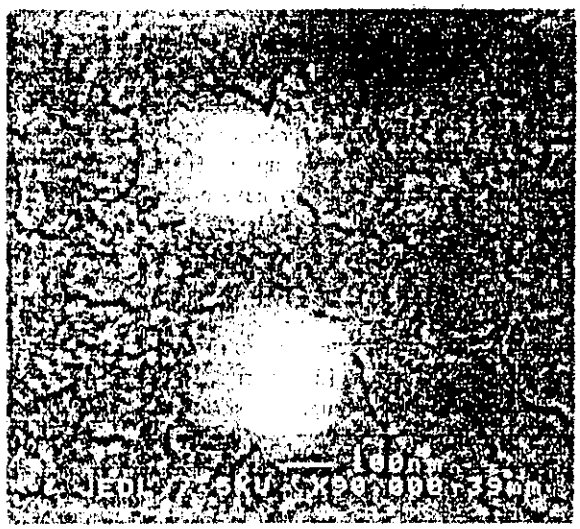

Figure 1 SEM photograph of the nano-scaled HAp particles.

m/u {Kluwer}Jmsm/Jmsm24/577003/577003.3d Date: 1/10/03 Time 14:10pm Page 2 of 5

where W_1 and W_2 are the dried MOI-modified SF and polyMPTS-grafted SF, respectively.

After HAp nano-scaled particles were suspended in toluene/methanol (9/1), a polyMPTS-grafted SF of 1.5 cm in diameter was soaked in the suspended solution for 1 h at room temperature to be adsorbed on the SF. The SF adsorbed with the particles was washed by stirring in methanol. This fabric with HAp was heated at 120 °C for 2 h in vacuum at 1 mmHg to react between the HAp particle and alkoxysilyl group of the grafted polymer. The composite was washed by using an ultrasonic generator for 3 min (output: 20 kHz, 35 W) to remove excess adsorbed HAp particles attached to those in the same solution. Finally, the composite was washed in a great amount of distilled water for 1 day to remove the residual organic solvents using the synthetic process.

To estimate the siloxane bond existing between HAp particles and the grafted substrate, a mixture product consisting of 90 mg of MPTS monomer and 10 mg of HAp particles was prepared. The mixture was treated at 120 °C for 2 h in vacuum (1 mmHg), according to the HAp coating process.

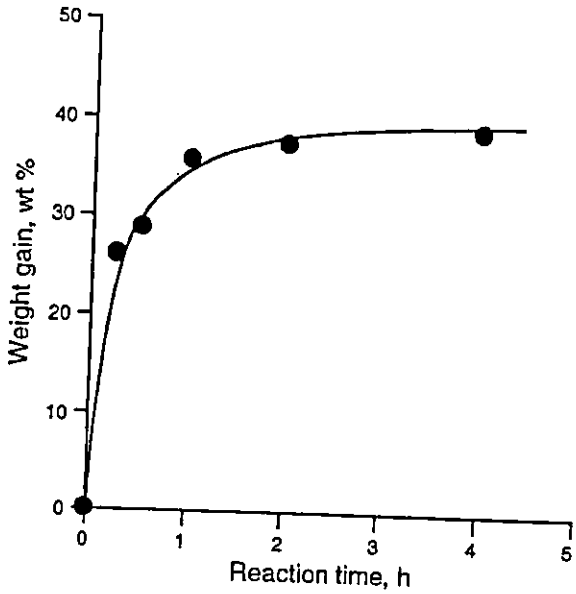

Figure 3 Weight gain of polyMPTS-grafted SF as a function of reaction time.

3. Results and discussion

The composite was prepared through a three-step procedure – the donation of vinyl groups on the SF as the first step, graft-polymerization of polyMPTS on the SF via the vinyl bonds as the second step, and coupling between HAp and the modified SF as the final step. The target of the amino acid in the SF for the donation of vinyl groups is hydroxyl residues because there are 10.6 mol % of Ser, 5.0 mol % of Tyr and 0.9 mol % of Thr in the amino acids of the SF. The isocyanate group of the MOI monomer predominantly reacts with primary alcohols using a di-n-butyltin (IV) dilaurate. Fig. 2 shows the ATR FT-IR spectra of the original SF, the MOI-modified SF and the polyMPTS grafted SF of 37.6 wt % of weight gain. Peaks at 1621, 1514 and 1260/1230 cm^{-1} were attributed to amide I, II, and III, respectively, which are the typical absorbance of the SF substrate in Fig. 2(a). After the modification with the MOI monomer, new peaks appeared at 1721 and 1163 cm^{-1} contributing carbonyl and ether groups of the monomer. The weak bands belonging to vinyl groups at 3095–3010 and 1690–1635 cm^{-1} cannot be observed in the FT-IR spectrum due to overlapping with the stronger bands of the SF substrate in Fig. 2(b) [9]. It has already been stated that the amount of MOI monomer donation could be well controlled by the reaction time [9]. Finally, additional peak at 1076 cm^{-1} attributed to Si–O–C appeared due to the graft-polymerization with polyMPTS in Fig. 2(c). The weight gain of polyMPTS on the SF was plotted as a function of the reaction time (Fig. 3). The weight gain of polyMPTS increased with increase in the reaction time, eventually reaching a plateau value of about 38 wt %. Compared to the amount of MOI monomer donation of 7.0–8.0 wt % to the original SF in the first step, the degree of the graft-polymerization in the next step is estimated relatively low by a simple calculation. The donated MOI monomer on SF fibers with large surface area was reasonable from the previous report [9]. There might be considerable vinyl groups that are unable to contribute to the graft-polymerization reaction in narrow spaces among fibers in the SF fabric. In the previous study, the weight gain of poly(2-methacryloyloxyethyl phosphorylcholine)-grafted on the SF through the same reaction system shows a plateau value that was about 26 wt % in a water/DMF mix solvent system [9]. The difference between these graft-polymerization efficiencies might depend on the solvent effect. The amount of the graft-polymerization on the SF could actually be well controlled in this system.

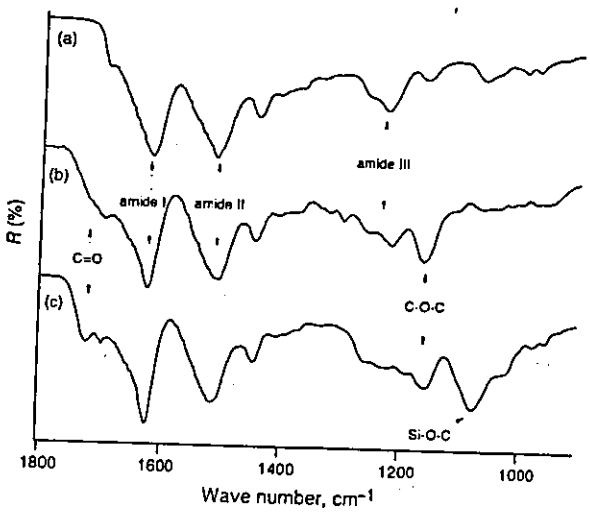

Figure 2 ATR FT-IR spectra of (a) original SF, (b) MOI-modified SF with 8.0 wt % of weight gain, and (c) polyMPTS-grafted SF with 33.8 wt %.

The existence of covalent bonds between the HAp particle and the polyMPTS-grafted SF was indirectly estimated by FT-IR (Fig. 4). The peak at 1076 cm^{-1} of the FT-IR spectrum was attributed to an Si–O–C stretching vibration of an alkoxysilyl group in the MPTS monomer (Fig. 4(a)). The peaks at 963 cm^{-1} reflected ν_1 PO_4^{3-} and 1100/1135 cm^{-1} for ν_3 PO_4^{3-} in

m/u (Kluwer)Jmsm/Jmsm24/577003/577003.3d Date: 1/10/03 Time 14:10pm Page 3 of 5

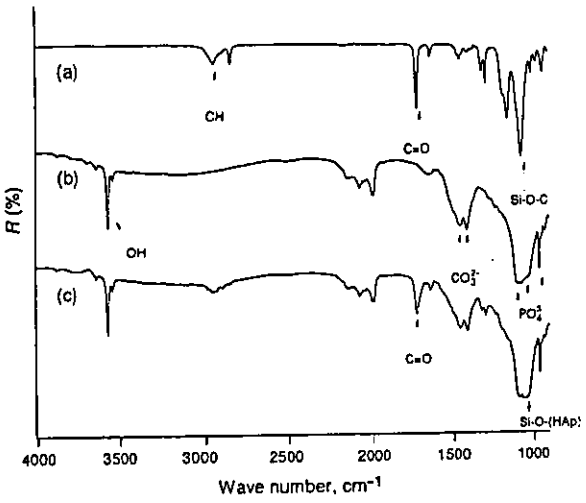

Figure 4 FT-IR spectra of (a) MPTS monomer. (b) original HAp particles, and (c) a heating product of a mixture of the HAp particles and MPTS monomer. The (a) and (b)/(c) spectra were analyzed by ATR and diffuse reflectance FT-IR, respectively.

Fig. 4(b). The strong peak at 3572 cm^{-1} was attributed to an OH stretching vibration which showed a well-crystallized product. The peaks at 1456 and 1412 cm^{-1} can be attributed to ν_3 CO_3^{2-}, which is known to be a better biomaterial due to its similarity to the composition of biological apatite. In the FT-IR spectrum (Fig. 4(c)) of the heating product of the mixture with the HAp particles and the MPTS monomer at 120 °C for 2 h in vacuum, a new peak appeared at 1043 cm^{-1}. This band is known as the sign belonging to an Si–O stretching vibration from the covalent bond between the HAp and the silane coupling agent [10]. The nano-particles actually remained on the surface of the SF substrate, even if the composite sustained considerable shear stress by an ultra-sonic vibration.

Fig. 5 shows the XRD patterns of the original SF (a) and HAp coating SF (b). The sharp peaks at 32° and 33° (2θ), attributed to (2 1 1) and (3 0 0) planes of HAp particles, newly appear in the XRD pattern (b) after the coating. This means that the highly crystalline inorganic material exists on the substrate surface. The peak at around 20° (2θ) shows the silk II form, β-sheet structure, in which crystalline regions of the SF fibers have an

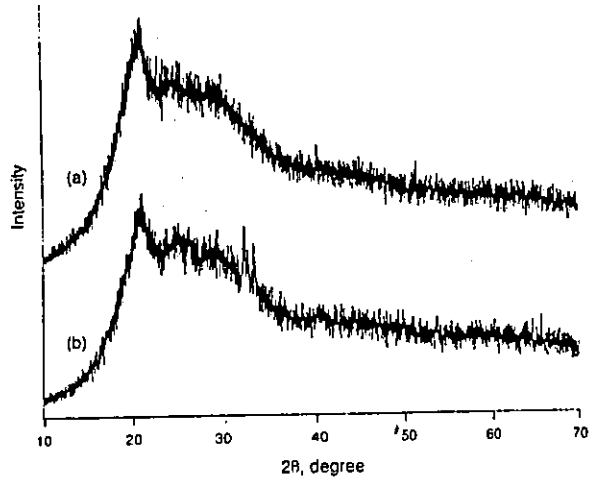

Figure 5 XRD patterns of (a) original SF and (b) the composite.

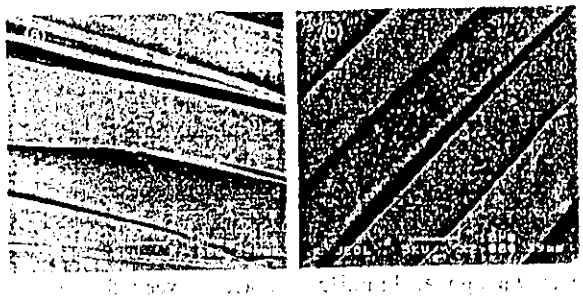

Figure 6 SEM photographs of (a) original SF surface after HAp adsorption and ultrasonic treatment, and (b) the composite surface.

identical orientation. There was no change in XRD patterns between the original SF and the composite except for the patterns of the HAp. This result shows that the crystalline structure of the SF substrate did not change after the heat applied to the HAp coating nor by the process of the graft-polymerization. This also means that the SF is able to withstand the severe condition of the reaction procedure, such as 120 °C for 2 h in vacuum. This phenomenon depends on the crystalline structure of the strong hydrogen bonding in antiparallel chain-pleated sheet structure consisting of a sequential polypeptide $[Ala–Gly]_n$ in the SF [11].

Fig. 6 shows the SEM photograph of the composite surface as well as the original SF surface conducted HAp adsorption and subsequent ultrasonic treatment. SF fibers of about 10 μm in width formed a parallel line. On the original SF, HAp particles were rarely observed due to the removal by ultrasonic treatment (Fig. 6(a)). The nano-particles separated or aggregated with several crystals, meanwhile, strongly remained on the treated SF surface, though some larger aggregates were removed by shear stress using an ultrasonic generator. It was very difficult to prepare a mono-layer adsorption of HAp crystals on the SF because the particles easily aggregate each other due to having ionic phases on the surface. A HAp crystal has two planes – the a- and c-plane. It is well known that the a- and c-plane show cationic and anionic charge, respectively [12]. We are now examining the adsorption behavior using a quartz crystal microbalance technique. Ionic charges of the HAp surface, moreover, might complexly influence against its bioactivity. In the former literature, the sintered HAp particle with an average diameter of 2 μm, that is the crystal aggregation, was used for cell adhesion and animal implantation [6]. The results show, eventually, the good bioactivity. The nano-HAp coating material thus presumes to possess good biocompatibility for soft tissue.

4. Conclusions

HAp nano-crystals below 200 nm in diameter were coated on the SF fibers, which were modified by polyMPTS-grafted polymers through vinyl groups. The graft-polymerization with polyMPTS was well controled by the reaction time. The nano-crystals were subsequently coated on the grafted fibers by heating at 120 °C for 2 h. The crystalline structure of the SF substrate did not change in the synthetic procedure. It was found that the bonded nano-crystals were separated and partially aggregated with several crystals on the fiber surface by SEM observation. The HAp crystals coated on the fibers

were not removed on the modified SF compared to the original one by ultrasonic treatment. The bioactivity of HAp could be applied to the polymer surface since this HAp resembles biological inorganic material. We are now developing three-dimensional material made of the HAp/SF composite aiming at a novel soft-tissue-compatible material.

References

1. H. AOKI, in "Medical Applications of Hydroxyapatite" (Ishiyaku EuroAmerica Inc., 1994) p. 90.
2. *ibid.* p. 133.
3. V. MIDY, C. REY, E. BRES and M. DARD, *J. Biomed. Mater. Res.* **41** (1998) 405.
4. M. Z. PAUL, M. C. CATHERINE, B. C. DOUGLAS and C. Y. A. RAYMOND, *ASAIO J.* **40** (1994) M896.
5. T. FURUZONO, K. SONODA and J. TANAKA, *J. Biomed. Mater. Res.* **56** (2001) 9.
6. T. FURUZONO, P. L. WANG, A. KOREMATSU, K. MIYAZAKI, M. OIDO-MORI, Y. KOWASHI, K. OHURA, J. TANAKA and A. KISHIDA, *J. Biomed. Mater. Res. (Appl. Biomater.)* **65B** (2003) 217.
7. T. FURUZONO, D. WALSH, K. SATO, K. SONODA and J. TANAKA, *J. Mater. Sci. Lett.* **20** (2001) 111.
8. K. SONODA, T. FURUZONO, D. WALSH, K. SATO and J. TANAKA, *Solid State Ionics* **151** (2002) 321.
9. T. FURUZONO, K. ISHIHARA, N. NAKABAYASHI and Y. TAMADA, *Biomaterials* **21** (2000) 327.
10. K. NISHIZAWA, M. TORIYAMA, T. SUZUKI, Y. KAWAMOTO, Y. YOKOGAWA and F. NATAGA, *Chem. Soc. Jpn.* **1** (1995) 63.
11. R. D. B. FRASER and T. P. MACRAE, in "Conformations of Fibrous Proteins and Related Synthetic Polypeptides" (Academic Press, New York, 1973) p. 293.
12. T. KAWASAKI, *J. Chromatogr.* **544** (1991) 147.

Received 20 January
and 29 July 2003

RAPID COMMUNICATION

Synthesis of a Novel Block Copolymer Containing Aromatic Polyamide and Fluoroethylene Segments

ARATA KOREMATSU, TSUTOMU FURUZONO, AKIO KISHIDA

Department of Biomedical Engineering, National Cardiovascular Center Research Institute, 5-7-1, Fujishirodai, Suita, Osaka 565-8565, Japan

Received 25 February 2003; accepted 30 June 2003
Published online 1 August 2003 in Wiley InterScience (www.interscience.wiley.com). DOI: 10.1002/pola.10872

Keywords: block copolymer; fluoroethylene; aromatic polyamide; polycondensation

INTRODUCTION

Recently, in the field of medicine, much attention has been paid to polymers with microphase-separated bulk and surface structures. Poly(2-hydroxyethyl methacrylate-styrene)[1] is well known as a biomedical block copolymer with good blood compatibility because of its microphase-separated structure. Segmented polyurethanes[2–4] and aramid–silicone resins[5] have also been developed as biomedical polymers with the same kind of structure. These polymers have not only good blood compatibility but also good mechanical properties. On the other hand, fluorinated polymers, such as poly(tetrafluoroethylene), exhibit a unique combination of high thermal stability, chemical inertness to solvents, hydrocarbons, acids, and alkalis, and high water repellency.[6–8] These polymers have major development roles in modern technologies. In the field of medical science, in particular, these polymers are applied to various biomedical devices, such as artificial vessels, because of their low bioactivity. It is expected that the development of a copolymer with the fluoroethylene segments and other functional segments will provide the realization of a novel functionality, such as the improvement of blood compatibility and mechanical properties.

We selected aromatic polyamides (aramids) as other functional segments of the fluorinated block copolymer because aramids have received considerable attention with respect to the production of high-performance materials on account of their outstanding thermal stability, chemical resistance, and mechanical properties.[9] The block copolymer with fluoroethylene and aramid segments is expected to form the microphase-separation structure easily because a distinct difference of polarity exists between fluorinated polymers and aramids. We report here the first attempt to synthesize the fluoroethylene–aramid block copolymer for the purpose of the development of a novel biomedical polymer. The characterization tests of the block copolymer were conducted with IR spectroscopy, ^{1}H NMR, and gel permeation chromatography (GPC).

EXPERIMENTAL

The synthesis of the telechelic diamine and the fluoroethylene–aramid block copolymer is outlined in Scheme 1.

Synthesis of the Telechelic Diamine

3,4′-Diaminodiphenylether (3,4′-DAPE; 4.00 g, 20 mmol; Wakayama Seika Kogyo Co., Ltd., Wakayama, Japan), 4.54 g (22 mmol) of 1,3-dicyclohexylcarbodiimide (DCC), and 20 mL of anhydrous *N,N′*-dimethylformamide (DMF) were placed in a thoroughly dried, 100-mL, three-necked, round-bottom flask equipped with a mechanical stirrer under a nitrogen atmosphere. After the solution was cooled with an ice bath, 1.90 g (10 mmol) of tetrafluorosuccinic acid (TFSA) and 3.24 g (24 mmol) of anhydrous 1-hydroxybenzotriazole (HOBt), previously dissolved in 20 mL of anhydrous DMF, were added slowly to the stirred solution. The reaction mixture was stirred for 1 h

Correspondence to: T. Furuzono (E-mail: furuzono@ri.ncvc.go.jp)

Journal of Polymer Science: Part A: Polymer Chemistry, Vol. 41, 2840–2845 (2003)